

Adaptive PCA for Time-Varying Data

Salaheddin Alakkari and John Dingliana
Graphics Vision and Visualisation Group (GV2)
School of Computer Science and Statistics
Trinity College Dublin
alakkars@tcd.ie|John.Dingliana@tcd.ie

December 14, 2024

Abstract

In this paper, we present an online adaptive PCA algorithm that is able to compute the full dimensional eigenspace per new time-step of sequential data. The algorithm is based on a one-step update rule that considers all second order correlations between previous samples and the new time-step. Our algorithm has $\mathcal{O}(n)$ complexity per new time-step in its deterministic mode and $\mathcal{O}(1)$ complexity per new time-step in its stochastic mode. We test our algorithm on a number of time-varying datasets of different physical phenomena. Explained variance curves indicate that our technique provides an excellent approximation to the original eigenspace computed using standard PCA in batch mode. In addition, our experiments show that the stochastic mode, despite its much lower computational complexity, converges to the same eigenspace computed using the deterministic mode.

1 Introduction

Principal Component Analysis (PCA) is one of the most important machine learning techniques for many reasons. Firstly, it is the only unsupervised learning algorithm that is theoretically proven to capture the maximal variability (information) of the input data given a fixed-size low-dimensional space. Another main reason is that it directly deals with the eigenspace of the problem on hand. In the real world, an endless amount of problems and physical phenomena can be modelled by eigenvalue equations. One important example is the Dirac equation which assumes that all variables of a physical object (speed, acceleration, etc) obey an eigenvalue problem [50]. In quantum physics, the quantum states that an electron in an atom can take (labeled as 1S, 2S, 2P etc) are actually time-dependent eigenfunctions which are called "quantum eigenstates" [56].

Despite the elegance of PCA, it has not been widely used until the last four decades. One reason for this is that, in its basic form, it has a quadratic space and time complexity which requires large memory and processing speed. Nowadays machines are shown to be more capable of solving such a problem thanks to the larger memory spaces and faster CPU and GPU units. However, for a wide range of problems where the dimensionality

of the data is massive (due to the size or number of samples), extracting the principal components in the standard way becomes infeasible. Many algorithms were developed to find the most significant principal components with linear complexity dependence on data size. However most of these approaches are stochastic and are limited to extracting a certain number of eigenvectors (principal components).

In this paper, we consider time-dependent systems that require regular monitoring and analysis for each new time-step. This is particularly important, for instance, in equilibria and stability analysis of the system. In many physical phenomena, such as the electron eigenstates example mentioned above, the time-dependent behavior of the significant eigenvectors converges to an equilibrium eigenstate. We propose an adaptive PCA algorithm that is able to capture all eigenvectors of the data and has $\mathcal{O}(n)$ complexity per new time-step in its deterministic mode and $\mathcal{O}(1)$ complexity per new time-step in its stochastic mode, where n is the number of previous time-steps. We test this algorithm on six time-varying datasets of different physical phenomena. We compare the performance of our algorithm with the standard PCA applied in batch-mode.

2 Background and Related Work

In the literature, there are two main directions that PCA research has taken. The first is that concerning applications which employ PCA for solving real-world problems and the second is that in the direction of PCA-optimization which is concerned with the optimization of the computational complexity of PCA. The link between the two directions is not clear since most studies in the application direction assume a pre-computed eigenspace and focus mainly on the distribution of test data in that eigenspace. On the other hand, in the optimization direction, the target use-case is not obvious. In addition, most of the optimization-direction algorithms are of a stochastic nature and are usually tested on rather simple datasets or data where a global eigenspace can be easily derived. In such a case, one can always consider a pre-computed eigenspace no matter what computational complexity was required for finding it. In fact, many online datasets provide a list of the most significant eigenvectors of the studied samples.

With regard to the applications research, the use of PCA has been well reported in the fields such as Computer Vision and Computer Graphics. For instance, in facial recognition, Kirby and Sirovich [29] proposed PCA as a holistic representation of the human face in 2D images by extracting few orthogonal dimensions which form the face-space and were called eigenfaces [60]. Gong et al. [23] were the first to find the relationship between the distribution of samples in the eigenspace, which were called manifolds, and the actual pose in an image of a human face. The use of PCA was extended using Reproducing Kernel Hilbert Spaces which non-linearly map the face-space to a much higher dimensional space (Hilbert space) [63]. Knittel and Paris [30] employed a PCA-based technique to find initial seeds for vector quantization in image compression. There are a number of previous reported uses of PCA-related methods in the computer graphics and visualization literature. For instance, Nishino et al. [43] proposed a method, called *Eigen-texture*, which creates a 3D image from a sample of range images using PCA.

They found that partitioning samples into smaller cell-images improved the rendering of surface-based 3D data. Grabner et al. [25] proposed a hardware accelerated technique that uses the multiple eigenspaces method [35] for image-based reconstruction of a 3D polygon mesh model. Liu et al. [36] employed PCA for dynamic projections in the visualization of multivariate data. Broersen et al. [11] discussed the use of PCA techniques in the generation of transfer functions, which are used to assign optical properties such as color and opacity to attributes in volume data. Takemoto et al. [57] used PCA for feature space reduction to support transfer function design and exploration of volumetric microscopy data. Fout and Ma [17] presented a volume compression method based on transform coding using the Karhunen-Lo  e Transform (KLT), which is closely related to PCA.

In the PCA-optimization research direction, the power iteration remains one of the most popular techniques for finding the top p eigenvectors [22]. In the recent literature, Shamir proposed a stochastic PCA algorithm that's proven to converge faster than the power iteration method [53]. Both techniques have a lower bound complexity of $\mathcal{O}(n \log(\frac{1}{\epsilon}))$ where ϵ is the precision of convergence. In addition, both techniques were experimentally tested to extract only a limited number of significant eigenvectors. Arora and De Sa et al. [15, 4, 5] proposed stochastic techniques that are based on the gradient-descent learning rule. The slow convergence rate of the gradient-descent rule is one main limitation of these techniques. Many algorithms were developed to find eigenvectors incrementally per new number of time-steps. Such techniques are referred to as incremental PCA algorithms. The update schemes proposed by Krasulina [32] and Oja [44] are the most popular incremental PCA techniques. Given a new time-step x_{n+1} and a significant eigenvector v for previous samples, the general update rule according to these techniques is

$$v^{i+1} = v^i + \alpha \langle x_{n+1}, v^i \rangle x_{n+1}; \quad v^{i+1} = \frac{v^{i+1}}{\|v^{i+1}\|},$$

where α is the learning rate. This process will keep updating until converging to a stable state. The speed of convergence of this technique is a matter of ongoing research. Balsubramani et al. [6] found that speed of convergence depends on the learning rate α . Another problem with this technique (as we will find later in this study) is that it does not consider change in weightings of previous time-steps. Mitiagkas et al. proposed an incremental PCA algorithm for streaming data with computational complexity of $\mathcal{O}(n \log(n))$ [41].

One important point to highlight is that most studies in both directions focus mainly on the most significant eigenvectors with little attention paid to the least significant ones. In fact, finding such eigenvectors was shown to play a key role in detecting outliers and non-belonging samples since they are perpendicular to the best fitting hyperplane. Jolliffe [28] pointed out in his book that the principal components corresponding to the smallest eigenvalues (variances) are not “unstructured left -overs” after extracting the higher PCs and that they can be useful in detecting outliers. The first use of the smallest PC in the literature was done by Gnanadesikan and Wilk 1969 [20]. Based on this work,

Gnanadesikan [21] stated that “with p -dimensional data, the projection onto the smallest principal component would be relevant for studying the deviation of an observation from a hyperplane of closest fit”. More recently, Izenman and Shen used the smallest kernel principal components for outlier detection as a generalization of the linear case [27]. Alakkari et al. found that the least significant eigenface can be used as a basis for discriminating between face and non-face images [3]. In Partial Differential Equations, many systems are solved by seeking a hyperplane that is constituted of the entire solution. This is known as the method of characteristics.

3 Concepts

The standard approach to PCA is as follows. Given data samples $X = [x_1 \ x_2 \ \cdots \ x_n] \in \mathbb{R}^{d \times n}$, where each sample is in column vector format, the covariance matrix is defined as

$$C = \frac{1}{n-1} \sum_{i=1}^n (x_i - \bar{x})(x_i - \bar{x})^T, \quad (1)$$

where \bar{x} is the sample mean. In the sequel of this paper, we will assume that all samples are centered and hence there is no need to subtract the sample mean explicitly. After computing the covariance matrix, we can find the optimal low-dimensional bases that cover most variability in samples by extracting the significant eigenvectors of the covariance matrix C . Eigenvectors are extracted by solving the following eigenvalue equation

$$(C - \lambda I)v = 0; \ v^T v = 1, \quad (2)$$

where $v \in \mathbb{R}^d$ is the eigenvector and λ is its corresponding eigenvalue. Eigenvalues describe the variance maintained by the corresponding eigenvectors. Hence, we are interested in the subset of eigenvectors that have the highest eigenvalues $V = [v_1 \ v_2 \ \cdots \ v_p]$; $p \ll n$. Then we encode a given sample x using its p -dimensional projection values (referred to as *scores*) as follows

$$W = V^T x. \quad (3)$$

We can then reconstruct the sample as follows

$$x_{\text{reconstructed}} = VW. \quad (4)$$

One advantage of PCA is the low computational complexity when it comes to encoding and reconstructing samples.

Duality in PCA

Since in the case of $n \ll d$, C will be of rank $n-1$ and hence there are only $n-1$ eigenvectors that can be extracted from Eq. (2) and since C is of size $d \times d$, solving Eq. (2) becomes computationally expensive. We can find such eigenvectors from the

dual eigenspace by computing the $n \times n$ matrix $X^T X$ and then solving the eigenvalue problem

$$(X^T X - (n-1)\lambda I) v_{dual} = 0 \quad (5)$$

$$\Rightarrow X^T X v_{dual} = (n-1)\lambda v_{dual}; v_{dual}^T v_{dual} = 1. \quad (6)$$

Here, for simplicity, we assumed that the sample mean of X is the zero vector. After extracting the dual eigenvectors, one can note that by multiplying each side of Eq. (6) by X , we have

$$\begin{aligned} X X^T X v_{dual} &= (n-1)\lambda X v_{dual} \\ \Rightarrow \frac{1}{n-1} X X^T (X v_{dual}) &= \lambda (X v_{dual}) \\ \Rightarrow C (X v_{dual}) &= \lambda (X v_{dual}) \\ \Rightarrow (C - \lambda I) (X v_{dual}) &= 0 \end{aligned}$$

which implies that

$$v = X v_{dual}. \quad (7)$$

Thus, when $n \ll d$, we only need to extract the dual eigenvectors using Eq. (6) and then compute the real eigenvectors using Eq. (7). Only the first few eigenvectors $V_p = [v_1 \ v_2 \ \dots \ v_p]$, $p \ll n \ll d$ will be chosen to represent the eigenspace, those with larger eigenvalues.

4 Adaptive PCA Algorithm

The main premise of our algorithm is based on the fact that an eigenvector is actually a weighted sum of the input samples. We can show that by rewriting Eq. (2) as follows

$$\begin{aligned} \left(\frac{1}{n-1} \sum_{i=1}^n x_i x_i^T - \lambda I \right) v &= 0 \\ \Rightarrow \frac{1}{n-1} \sum_{i=1}^n x_i x_i^T v - \lambda v &= 0 \\ \Rightarrow \frac{1}{n-1} \sum_{i=1}^n x_i \langle x_i, v \rangle - \lambda v &= 0 \\ \Rightarrow v &= \frac{1}{\lambda(n-1)} \sum_{i=1}^n \langle x_i, v \rangle x_i. \end{aligned}$$

A first guess for an update formula given new time-step x_{n+1} would be

$$v^{t+1} = v^t + \langle x_{n+1}, v^t \rangle x_{n+1}; \quad v^{t+1} = \frac{v^{t+1}}{\|v^{t+1}\|}.$$

This is similar to Oja's update scheme mentioned in the background section. The problem with this formula is that it assumes the weightings of previous samples are fixed. As the eigenvector is updated for each new time-step, the weights of previous samples should also be adjusted according to their projections on the updated eigenvector. The change in weights will be proportional to the correlations between previous samples and the new time-step. In our algorithm we used the following update rule

$$\begin{aligned}
v^{t+1} &= v^t + \left(\sum_{j=1}^n \langle v^t, x_j \rangle \langle x_j, x_{n+1} \rangle^2 x_j \right) + \langle v^t, x_{n+1} \rangle \left(\sum_{j=1}^{n+1} \langle x_j, x_{n+1} \rangle \right)^2 x_{n+1} \\
&= v^t + \left(\sum_{j=1}^n \langle v^t, x_j \rangle \langle x_j, x_{n+1} \rangle^2 x_j \right) \\
&\quad + \langle v^t, x_{n+1} \rangle \left(\sum_{j=1}^{n+1} \sum_{i=1}^{n+1} \langle x_j, x_{n+1} \rangle \langle x_i, x_{n+1} \rangle \right) x_{n+1}; \quad v^{t+1} = \frac{v^{t+1}}{\|v^{t+1}\|}.
\end{aligned}$$

Unlike Oja's method, this is an online scheme that adapts weightings of all previous samples based on the squared dot product with the new time-step. In addition, the new time-step is weighted based on the sum of all second order dot products $\{\langle x_i, x_{n+1} \rangle \cdot \langle x_j, x_{n+1} \rangle\}_{i,j=1}^{n+1}$ multiplied by new time-step's score $\langle v^t, x_{n+1} \rangle$. Since for each eigenvector, we are computing the correlations (dot products) between the new time-step x_{n+1} and all n previous samples and considering that scores (weights) of previous samples $\{\langle v^t, x_j \rangle\}_{j=1}^n$ are computed in the previous iteration, this requires a time complexity of $\mathcal{O}(n)$ dot products per eigenvector per new time-step.

The full pseudo-code of our algorithm is shown in Algorithm 1. There are two parameters used in our algorithm: *space_limit* which specifies the maximal number of significant eigenvectors to compute and *processing_limit* which specifies the maximal number of dot products to compute per new time-step per eigenvector. As we mentioned earlier, our algorithm is capable of finding all eigenvectors of the data. In order to compute the full dimensional eigenspace deterministically, we set *space_limit* = $\min(d, n)$ and *processing_limit* $\gg n$ where d is the total number of dimensions per sample and n is the current number of samples. In its full-dimensional mode, our algorithm starts with two time-steps with $\frac{x_2 - x_1}{\|x_2 - x_1\|}$ as the initial eigenvector and ends with the full-dimensional eigenspace of the data. Line 10 of the algorithm includes the general update rule. Line 11 is used particularly for the limited processing mode (stochastic mode) to stress the shared information learned by v^t and v^{t+1} . Line 13 performs Gram-Schmidt process to ensure that following update terms will be orthogonal to updated eigenvector. After finishing the loop, \tilde{X} will constitute the n th eigenvector since it will be perpendicular to all $n - 1$ updated components.

Algorithm 1: Adaptive PCA

```
1 for each new time-step  $x_{n+1}$  do
2    $X = [X, x_{n+1}]$ ;
3    $\tilde{X} = X$ ;
4   if  $n > processing\_limit$  then
5     |  $indices = \text{rand}(n, processing\_limit)$ ;
6   else
7     |  $indices = 1 : n$ ;
8   end
9   for  $i = 1 : (\min(n, space\_limit) - 1)$  do
10    |  $\tilde{v} = v_i + \left( \sum_{j=indices} \langle v_i, \tilde{x}_j \rangle \langle \tilde{x}_j, \tilde{x}_{n+1} \rangle^2 \tilde{x}_j \right) +$ 
11      |  $\langle v_i, \tilde{x}_{n+1} \rangle \left( \left( \sum_{j=indices} \langle \tilde{x}_j, \tilde{x}_{n+1} \rangle \right) + \langle \tilde{x}_{n+1}, \tilde{x}_{n+1} \rangle \right)^2 \tilde{x}_{n+1}$ ;
12    |  $v_i = \tilde{v} + \langle \tilde{v}, v_i \rangle v_i$ ;
13    |  $v_i = \frac{v_i}{\|v_i\|}$ ;
14    |  $\tilde{X}_{indices \cup \{n+1\}} = \tilde{X}_{indices \cup \{n+1\}} - v_i \left( v_i^T \tilde{X}_{indices \cup \{n+1\}} \right)$ ;
15   end
16    $v_{\min(n, space\_limit)} = \sum_{j=indices \cup \{n+1\}} \tilde{x}_j$ ;
17    $n = n + 1$ ;
18 end
```

4.1 Limited-Dimensional Adaptive PCA

In the limited dimensional mode of our algorithm, we set a maximal number of eigenvectors to update/compute per new time-step using the *space_limit* parameter. Since this parameter value is constant throughout the execution of our algorithm, this will bound the time complexity to $\mathcal{O}(\text{space_limit} \times n) = \mathcal{O}(n)$ dot products per new time-step.

4.2 Limited-Dimensional Adaptive PCA in Stochastic Mode

In the stochastic mode, we specify a maximal number of dot products to be computed per new time-step per eigenvector. This happens when $n > \text{processing_limit}$. In this case, we choose *processing_limit* uniformly distributed random samples to compute their dot products with the new time-step. This will further bound the time complexity to $\mathcal{O}(\text{space_limit} \times \text{processing_limit}) = \mathcal{O}(1)$ dot products per new time-step. Considering that our algorithm does not require the computation of the covariance matrix, the full time complexity of PCA in the stochastic mode will be $\mathcal{O}(n)$ dot products (after processing all time-steps of the input data).

5 Experimental Results

We applied our algorithm on six time-varying datasets of different physical phenomena. The first dataset studies the stages of a supernova during a period of less than one second after a star's core collapses [10]. The second dataset studies the fluid dynamics in turbulent vortex in a 3D area of the fluid [55]. The third dataset shows the evolution of splash caused after a drop impact on liquid surface [58]. The fourth dataset was generated to analyze the chaotic path of a drop of silicone oil bouncing on the surface of a vibrating bath of the same material [45]. The fifth experimental data shows the unusual behaviour of some particles self-organized into spirals after rotational fluid flow [48]. Finally, the sixth dataset shows the behaviour of nitrogen bubbles cascading down the side of a glass of dark beer, which has been well-investigated in a number of papers [7, 47]. Table 1 summarizes the properties of each dataset. The first two datasets are in the form a 3D scalar field (i.e. voxels datasets). The remaining four datasets are in video format and were adapted from original sources by converting to greyscale video frames and cropping these frames to a segment of interest (the most highly varying part of the video sequence). The adapted datasets can be obtained by emailing the authors.

We compare between the performance of our algorithm and standard PCA in terms of explained variance curves. The standard PCA results are generated using the *pcacov* function in MATLAB [39]. Since we are dealing with cases where $n \ll d$, it is typical to use the dual covariance matrix $X^T X$ for standard PCA. For the adaptive PCA, we incrementally update the eigenvectors until reaching the last time-step as in Algorithm 1.

We first compare between the full-dimensional eigenspace computed using each technique. This is to stress the capability of our approach of finding all eigenvectors of the given datasets. Figure 1 shows the explained variance curves of each dataset. It's

Table 1: Summary of the datasets used in our experiments.

dataset/experiment name	data type	time-step resolution	number of time-steps
Supernova	3D volumes	432^3 voxels	60
Turbulent Vortex	3D volumes	128^3 voxels	100
Droplet Impact on Liquid Surface	grayscale video	240×312 pixels	100
Bouncing Silicone Drop	grayscale video	300×640 pixels	300
Self Organized Particles	grayscale video	54×152 pixels	650
Guinness Cascade	grayscale video	271×131 pixels	1,100

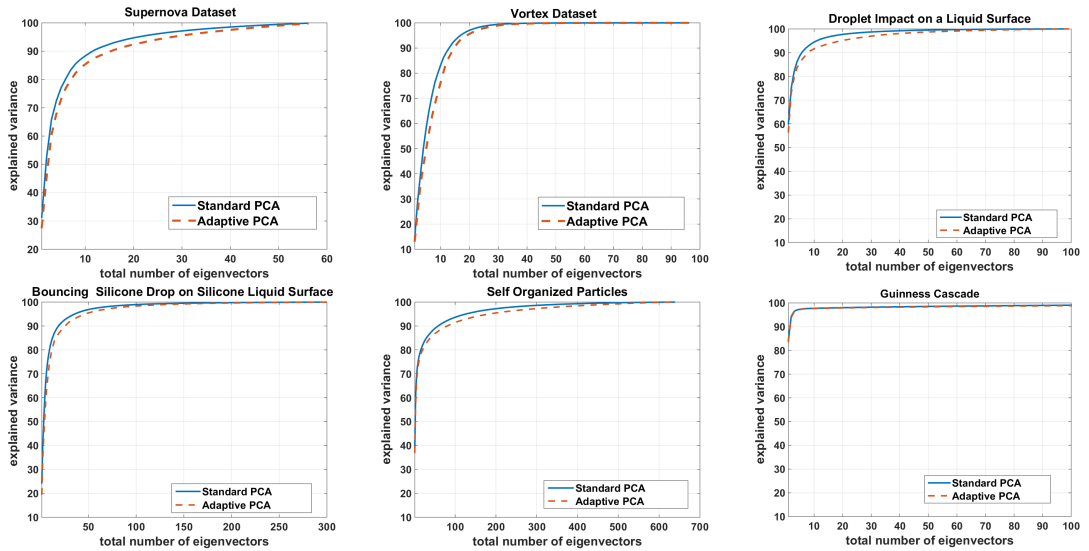


Figure 1: Explained variance curves of standard PCA and full-dimesional adaptive PCA for each dataset.

very clear how our algorithm provides an excellent approximation to the original full-dimensional eigenspace. For all datasets, the gap between the two curves does not exceed 2%. It's also interesting to note how both techniques well-learned the guinness cascade phenomenon where 98% of the variability was covered by only the first 20 eigenvectors.

Now, we shall compute the limited-dimensional eigenspace for each dataset to mainly compare performance between deterministic and stochastic modes of our algorithm. Figure 2 shows the performance of the 20-dimensional adaptive PCA. To test the stochastic mode performance, we applied 10 runs of our algorithm where in each run we set *processing_limit* to 40. With much lower number of computations, the stochastic runs are providing almost the same performance as the deterministic mode. The only difference one can note is in the *Self Organized Particles* experiment where the stochastic runs provide mean explained variance of 77% while the deterministic mode covers 80% of variability.

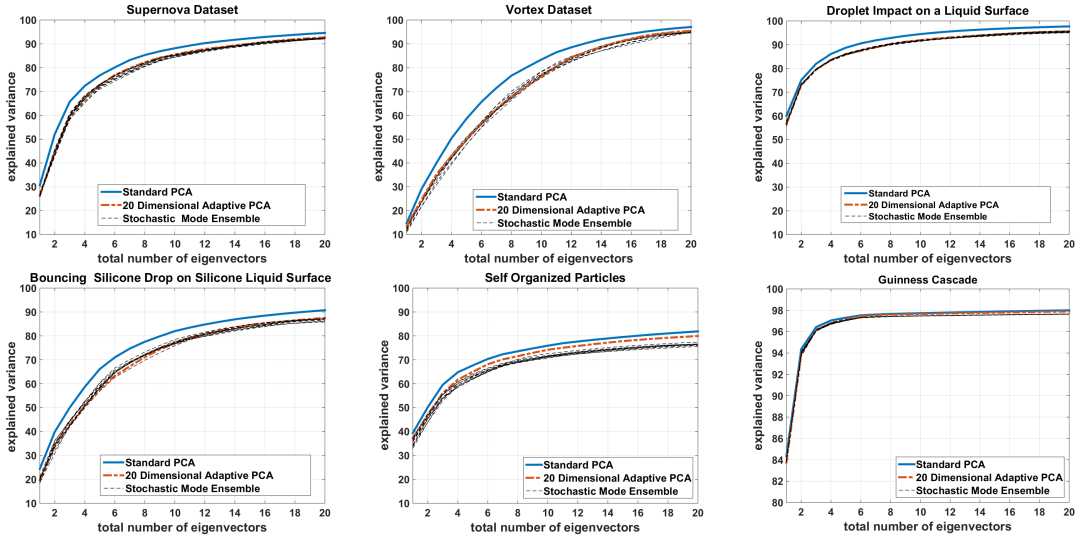


Figure 2: Explained variance curves of standard PCA and 20-dimensional adaptive PCA in both deterministic and stochastic modes for each dataset.

6 Conclusion

In this paper, we presented a deterministic scheme that finds the eigenspace of sequential data incrementally with linear time complexity growth. Our model is a generalization of Oja’s method with the following two main advantages. In our approach, the eigenvectors are updated in an online manner (one-step update per eigenvector) unlike Oja’s method which is applied in an iterative manner per eigenvector. Secondly, our model considers all previous samples in its update formula whereas Oja’s method considers only the most recent time-step in its update rule. Since our algorithm considers all second order correlations between samples, this provides an intensive learning scheme that better resembles the quadratic nature of standard PCA. In the limited-computations mode of our algorithm (stochastic mode), the eigenvectors are adapted according to the pattern learned from limited population ensembles. Our experiments have shown that the stochastic mode provides the same performance as the deterministic mode with much lower number of computations. Our technique serves as a robust modeling tool for complex time-dependent systems that decomposes the systems temporal behaviour using orthogonal time-dependent functions which correspond to the dual eigenspace. This can be expressed as follows

$$\vec{S}_t = \sum_{i=1}^p v_i f_i(t) = \sum_{i=1}^p v_i (v_i^T x_t).$$

Figures 3 shows the time-dependent functions of the first, fifth and tenth eigenvectors for the Supernova and Vortex datasets. One can note that the higher significance eigenfunctions have lower frequency with higher amplitude. By interpolating these functions, we can analyze the system behavior in continuous time. In terms of future work, it would

be interesting to know the performance of our algorithm using different distributions of previous samples in the stochastic mode. In many systems, the recent samples have higher priority than older ones, such as in CCTV surveillance applications where the records are saved for a limited period of time.

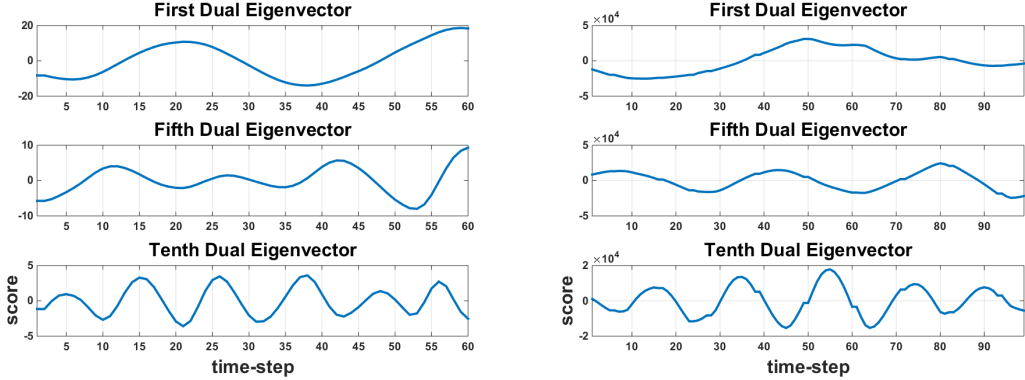


Figure 3: Three time-dependent eigenvectors for Supernova (left) and Vortex (right) datasets.

Acknowledgments

This research has been conducted with the financial support of Science Foundation Ireland (SFI) under Grant Number 13/IA/1895.

References

- [1] Salaheddin Alakkari and John Dingliana. Volume Rendering Using Principal Component Analysis. In Tobias Isenberg and Filip Sadlo, editors, *EuroVis 2016 - Posters*. The Eurographics Association, 2016.
- [2] Salaheddin Alakkari and John Dingliana. Volume Visualization Using Principal Component Analysis. In Stefan Bruckner, Bernhard Preim, Anna Vilanova, Helwig Hauser, Anja Hennemuth, and Arvid Lundervold, editors, *Eurographics Workshop on Visual Computing for Biology and Medicine*. The Eurographics Association, 2016.
- [3] Salaheddin Alakkari, Eugene Gath, and John James Collins. An investigation into the use of subspace methods for face detection. In *Neural Networks (IJCNN), 2015 International Joint Conference on*, pages 1–7. IEEE, 2015.
- [4] Raman Arora, Andrew Cotter, Karen Livescu, and Nathan Srebro. Stochastic optimization for PCA and PLS. In *Communication, Control, and Computing (Allerton), 2012 50th Annual Allerton Conference on*, pages 861–868. IEEE, 2012.

- [5] Raman Arora, Andy Cotter, and Nati Srebro. Stochastic optimization of PCA with capped MSG. In *Advances in Neural Information Processing Systems*, pages 1815–1823, 2013.
- [6] Akshay Balsubramani, Sanjoy Dasgupta, and Yoav Freund. The fast convergence of incremental PCA. In *Advances in Neural Information Processing Systems*, pages 3174–3182, 2013.
- [7] ES Benilov, CP Cummins, and WT Lee. Why do bubbles in guinness sink? *American Journal of Physics*, 81(2):88–91, 2013.
- [8] Wes Bethel. Visualization dot com. *IEEE Computer Graphics and Applications*, 20(3):17–20, 2000.
- [9] Clemens Birklbauer and Oliver Bimber. Light-field supported fast volume rendering. In *ACM SIGGRAPH 2012 Posters*, SIGGRAPH ’12, pages 125:1–125:1, New York, NY, USA, 2012. ACM.
- [10] J. Blondin. Supernova dataset. <http://vis.cs.ucdavis.edu/VisFiles/pages/supernova.php>.
- [11] Alexander Broersen, Robert van Liere, and Ron M.A. Heeren. Comparing three PCA-based methods for the visualization of imaging spectroscopy data. In *Proceedings of the Fifth IASTED International Conference on Visualization, Imaging and Image Processing*, pages 540–545, September 2005.
- [12] Steven P Callahan, Louis Bavoil, Valerio Pascucci, and Claudio T Silva. Progressive volume rendering of large unstructured grids. *IEEE Transactions on Visualization and Computer Graphics*, 12(5):1307–1314, 2006.
- [13] Baoquan Chen, Arie Kaufman, and Qingyu Tang. *Image-Based Rendering of Surfaces from Volume Data*, pages 279–295. Springer Vienna, Vienna, 2001.
- [14] Jae-Jeong Choi and Yeong Gil Shin. Efficient image-based rendering of volume data. In *Computer Graphics and Applications, 1998. Pacific Graphics ’98. Sixth Pacific Conference on*, pages 70–78, 226, Oct 1998.
- [15] Christopher De Sa, Kunle Olukotun, and Christopher Ré. Global convergence of stochastic gradient descent for some non-convex matrix problems. *arXiv preprint arXiv:1411.1134*, 2014.
- [16] Klaus Engel and Thomas Ertl. Texture-based volume visualization for multiple users on the world wide web. In *Virtual Environments*, pages 115–124. 1999.
- [17] N. Fout and K. L. Ma. Transform coding for hardware-accelerated volume rendering. *IEEE Transactions on Visualization and Computer Graphics*, 13(6):1600–1607, Nov 2007.

- [18] S. Frank and A. Kaufman. Distributed volume rendering on a visualization cluster. In *Ninth International Conference on Computer Aided Design and Computer Graphics (CAD-CG'05)*, Dec 2005.
- [19] G. Frieder, D. Gordon, and R. A. Reynolds. Back-to-front display of voxel based objects. *IEEE Computer Graphics and Applications*, 5(1):52–60, Jan 1985.
- [20] R Gnanadesikan and MB Wilk. Data analytic methods in multivariate statistical analysis. *Multivariate analysis*, 2:593–638, 1969.
- [21] Ramanathan Gnanadesikan and John R Kettenring. Robust estimates, residuals, and outlier detection with multiresponse data. *Biometrics*, pages 81–124, 1972.
- [22] Gene H Golub and Charles F Van Loan. *Matrix computations*, volume 3. JHU Press, 2012.
- [23] Shaogang Gong, Stephen McKenna, and John J Collins. An investigation into face pose distributions. In *Automatic Face and Gesture Recognition, 1996., Proceedings of the Second International Conference on*, pages 265–270. IEEE, 1996.
- [24] Nicolas Gourier, Daniela Hall, and James L Crowley. Estimating face orientation from robust detection of salient facial features. In *ICPR International Workshop on Visual Observation of Deictic Gestures*. Citeseer, 2004.
- [25] M Grabner, H Bischof, Ch Zach, and A Ferko. Multiple eigenspaces for hardware accelerated image based rendering. *in Proceedings of ÖAGM*, pages 111–118, 2003.
- [26] Markus Hadwiger, Joe M. Kniss, Christof Rezk-salama, Daniel Weiskopf, and Klaus Engel. *Real-time Volume Graphics*. A. K. Peters, Ltd., Natick, MA, USA, 2006.
- [27] Alan J Izenman and Yan Shen. Outlier detection using the smallest kernel principal components. *Astro Temple Edu, pdf report*, 2009.
- [28] Ian Jolliffe. *Principal component analysis*. Wiley Online Library, 2002.
- [29] M. Kirby and L. Sirovich. Application of the karhunen-loeve procedure for the characterization of human faces. *Pattern Analysis and Machine Intelligence, IEEE Transactions on*, 12(1):103–108, 1990.
- [30] G. Knittel and R. Parys. PCA-based seeding for improved vector quantization. In *Proceedings of the First International Conference on Computer Imaging Theory and Applications (VISIGRAPP 2009)*, pages 96–99, 2009.
- [31] Peter Kohlmann, Tobias Boskamp, Alexander Köhn, Christian Rieder, Andrea Schenk, Florian Link, Uwe Siems, Marcus Barann, Jan-Martin Kuhnigk, Daniel Demedts, and Horst K. Hahn. *Remote Visualization Techniques for Medical Imaging Research and Image-Guided Procedures*, pages 133–154. Springer International Publishing, Cham, 2016.

- [32] TP Krasulina. A method of stochastic approximation for the determination of the least eigenvalue of a symmetric matrix. *Zhurnal Vychislitel'noi Matematiki i Matematicheskoi Fiziki*, 9(6):1383–1387, 1969.
- [33] Thomas Kroes, Frits H Post, and Charl P Botha. Exposure Render: An interactive photo-realistic volume rendering framework. *PLoS ONE*, 8, 2013.
- [34] Philippe Lacroute and Marc Levoy. Fast volume rendering using a shear-warp factorization of the viewing transformation. In *Proceedings of the 21st Annual Conference on Computer Graphics and Interactive Techniques*, SIGGRAPH '94, pages 451–458, New York, NY, USA, 1994. ACM.
- [35] A. Leonardis and H. Bischof. Multiple eigenspaces by mdl. In *Proceedings 15th International Conference on Pattern Recognition. ICPR-2000*, volume 1, pages 233–237 vol.1, 2000.
- [36] S. Liu, B. Wang, J. J. Thiagarajan, P. T. Bremer, and V. Pascucci. Multivariate volume visualization through dynamic projections. In *2014 IEEE 4th Symposium on Large Data Analysis and Visualization (LDAV)*, pages 35–42, Nov 2014.
- [37] Rafat Mantiuk, Kil Joong Kim, Allan G Rempel, and Wolfgang Heidrich. Hdr-vdp-2: a calibrated visual metric for visibility and quality predictions in all luminance conditions. In *ACM Transactions on Graphics (TOG)*, volume 30, page 40. ACM, 2011.
- [38] The Mathworks, Inc., Natick, Massachusetts. *MATLAB version 8.5.0.197613 (R2015a)*, 2015.
- [39] The Mathworks, Inc., Natick, Massachusetts. *MATLAB and Statistics Toolbox Release 2017a*, 2017.
- [40] Miriah Meyer, Hanspeter Pfister, Charles Hansen, Chris Johnson, Miriah Meyer, Hanspeter Pfister, Charles Hansen, and Chris Johnson. Image-based volume rendering with opacity light fields. Technical report, University of Utah, 2005.
- [41] Ioannis Mitliagkas, Constantine Caramanis, and Prateek Jain. Memory limited, streaming pca. In *Advances in Neural Information Processing Systems*, pages 2886–2894, 2013.
- [42] Manuel Moser and Daniel Weiskopf. Interactive volume rendering on mobile devices. In *Vision, Modeling, and Visualization VMV*, volume 8, pages 217–226, 2008.
- [43] Ko Nishino, Yoichi Sato, and Katsushi Ikeuchi. Eigen-texture method: Appearance compression based on 3D model. In *Computer Vision and Pattern Recognition, 1999. IEEE Computer Society Conference on.*, volume 1. IEEE, 1999.
- [44] E OJE. Subspace methods of pattern recognition. In *Pattern recognition and image processing series*, volume 6. Research Studies Press, 1983.

[45] S Perrard, E Fort, and Y Couder. Wave-based turing machine: Time reversal and information erasing. *Physical review letters*, 117(9):094502, 2016.

[46] A. V. Poliakov, , E. Albright, D. Corina, G. Ojemann, R.F. Martin, and J.F. Brinkley. Server-based approach to web visualization of integrated 3D medical image data. In *Proceedings of the AMIA Symposium*, pages 533–537, 2001.

[47] OA Power, W Lee, AC Fowler, P Dellar, LW Schwartz, S Lukaschuk, G Lessells, AF Hegarty, M O’Sullivan, and Y Liu. The initiation of guinness. 2009.

[48] DO Pushkin, DE Melnikov, and VM Shevtsova. Ordering of small particles in one-dimensional coherent structures by time-periodic flows. *Physical review letters*, 106(23):234501, 2011.

[49] Xiaojun Qi and John M Tyler. A progressive transmission capable diagnostically lossless compression scheme for 3D medical image sets. *Information Sciences*, 175(3):217–243, 2005.

[50] Carlo Rovelli. *Quantum gravity*. Cambridge university press, 2007.

[51] A.P. Santhanam, Y. Min, T.H. Dou, P. Kupelian, and D. A. D.A. Low. A client-server framework for 3D remote visualization of radiotherapy treatment space. *Frontiers in Oncology*, 3, 2013.

[52] Nicole Schubert and Ingrid Scholl. Comparing GPU-based multi-volume ray casting techniques. *Computer Science - Research and Development*, 26(1):39–50, 2011.

[53] Ohad Shamir. A stochastic pca and svd algorithm with an exponential convergence rate. In *ICML*, pages 144–152, 2015.

[54] Alok Sharma and Kuldip K. Paliwal. Fast principal component analysis using fixed-point algorithm. *Pattern Recogn. Lett.*, 28(10):1151–1155, July 2007.

[55] D. Silver. Turbulent vortex dataset. <http://www.cs.ucdavis.edu/~ma/ITR>. Available from the Time-varying data repository at UC Davis.

[56] Walter Fox Smith. *Waves and oscillations: a prelude to quantum mechanics*. Oxford University Press, 2010.

[57] Shintaro Takemoto, Megumi Nakao, Tetsuo Sato, Tadao Sugiura, Kotaro Minato, and Tetsuya Matsuda. Interactive volume visualization of microscopic images using feature space reduction. *BME*, 51:U–6–U–6, 2013.

[58] Marie-Jean Thoraval, Kohsei Takehara, Takeharu Goji Etoh, Stéphane Popinet, Pascal Ray, Christophe Josserand, Stéphane Zaleski, and Sigurdur T Thoroddsen. von kármán vortex street within an impacting drop. *Physical review letters*, 108(26):264506, 2012.

- [59] Anna Tikhonova, Carlos D Correa, and Kwan-Liu Ma. Explorable images for visualizing volume data. In *IEEE Pacific Visualization Symposium*, pages 177–184, 2010.
- [60] Matthew Turk and Alex Pentland. Eigenfaces for recognition. *Journal of cognitive neuroscience*, 3(1):71–86, 1991.
- [61] Zhou Wang, A. C. Bovik, H. R. Sheikh, and E. P. Simoncelli. Image quality assessment: from error visibility to structural similarity. *IEEE Transactions on Image Processing*, 13(4):600–612, April 2004.
- [62] Satoshi Watanabe and Nikhil Pakvasa. Subspace method in pattern recognition. In *Proc. 1st. IJCPR*, pages 25–32, 1973.
- [63] M. H. Yang. Kernel eigenfaces vs. kernel fisherfaces: Face recognition using kernel methods. In *Proceedings of Fifth IEEE International Conference on Automatic Face Gesture Recognition*, pages 215–220, May 2002.